

Numerical Simulation of Substation Grounding Grids Buried in Vertical Earth Model Based on the Thin-Wire Approximation with Linear Basis Functions

Zhong-Xin Li, Guang-Fan Li, Jian-Bin Fan, and Yu Yin

Department of High Voltage
China Electrical Research Institute, Beijing, China
lizx@epri.sgcc.com.cn, ligf@epri.sgcc.com.cn, fanjb@epri.sgcc.com.cn, yiny@epri.sgcc.com.cn

Abstract — In order to improve the precision of the numerical result, the fast convergent Galerkin's type of boundary element method (BEM) with one order basis function is developed to calculate the grounding system buried in the vertical multilayer earth model. In this paper, the method is taken to simulate and analyze a grounding system including a floating electrode with any complicated structure, which can be located anywhere in the vertical multilayer earth model. The quasi-static complex image method (QSCIM) and the closed form of Green's function for the vertical multilayer earth model are introduced; the QSCIM is implemented by the matrix pencil (MP) approach.

Index Terms — Boundary element method, grounding system, quasi-static complex image method.

I. INTRODUCTION

There have been lots of papers researching the transient performance of AC substation grounding systems [1-8]; meanwhile, there also have been many papers studying the steady performance of AC substation grounding systems, especially in the low-frequency domain (about 50 to 60 Hz) [9-29]. This paper focuses on steady performance in low frequency of the AC substation grounding systems. References [9-17] are based on the unequal potential mathematical model, and references [18-29] are based on the equipotential mathematical model. In this paper, only the equipotential mathematical models for grounding problems buried in the vertical multilayer earth model will be discussed, and we can observe these equipotential mathematical model references [18-

29] with some variations: electrostatic theory is used in [18-26], while quasi-static electric field theory is used in [27-29]. For grounding problems in the vertical earth model case at a low frequency domain, [17] discusses the grounding problem based on an unequal potential mathematical model; however, [27-29] discusses the grounding problem basing on equal potential mathematical model.

In the papers [27 and 28], the infinite Maclaurin series is used to expand the integral kernel of Green's function of a Hertz dipole to avoid infinite integrals about Bessel function. Meanwhile, the complex image method based on the same Maclaurin's series expansion has been studied for horizontal multilayer earth model in the early references [30 and 31]. To avoid an infinite series, a method named quasi-static complex image for horizontal and vertical multilayer earth model is used in references [13-17, and 29]. It points out that the integral kernel of Green's function can be expanded to the finite exponential term series, and hence, the complex image method requires only four to six images to obtain accurate results.

BEM for solving the grounding system problem has been pioneer researched in [25 and 26]. However, the applications of the BEM for grounding systems are also based on the direct current electrical field theory. The BEM has been developed to calculate the AC grounding system's problem based on the quasi-static electrical field theory in paper [29], recently. However, the zero order basis function is used in paper [29].

To improve the precision of numerical results, a hybrid with the closed form of Green's function of the vertical multilayer earth model, fast

convergent Galerkin's type of the BEM combined with one order basis function is developed in this paper, the QSCIM and the closed form of Green's function for vertical multilayer earth model are introduced, and the QSCIM is implemented by the MP approach. So it can be used to calculate the currents distribution along both the grounding system and the floating metallic conductors buried in the vertical multilayer earth model; meanwhile, not only the conductive effect of current leaking into the vertical multilayer earth model, but also capacitive effects from the vertical multilayer earth model, have been considered in the method.

II. THE BASIS OF THE SIMULATION METHOD

A. 2D BEM

In the numerical simulation of the grounding system including a floating electrode buried in N_s -layer earth model, the grounding system including the floating electrode is divided into small cylindrical segments. First, supposing the system consists of total N_l segments of cylindrical bars. Then, considering the leakage currents density J_i ($i=1, \dots, N_l$) emanating from the surface of each segment as unknowns. Next, constructing an equation system, and supposing the grounding system and floating electrode are equipotential, and the scalar electrical potential (SEP) of each segment are also unknown. In this way, by solving the equation system, the currents can be obtained. Finally, the SEP at any point can be calculated by the contributions of all the currents.

From [25, 29, and 35], applying BEM, we have weighted the residual method as

$$\begin{aligned} & \int_{S_j} \sum_{m=1}^M W_m^{(s)}(\bar{r}) \varphi_j(\bar{r}) dS_j \\ &= \sum_{i=1}^{N_l} \int_{S_i} \sum_{m=1}^M W_m^{(s)}(\bar{r}) \int_{S_i'} G_\phi(\bar{r}, \bar{r}') \sum_{n=1}^M J_n N_n^{(s)}(\bar{r}') dS_i' dS_j. \end{aligned} \quad (1)$$

Here, $j=1, \dots, N_l$, S_i and S_j are the surfaces of i th and j th segments, dS_i' and dS_j are the infinite small surface elements of the cylindrical segments. Both basis functions and weight function $\{N_n^{(s)}(\bar{r}'), W_m^{(s)}(\bar{r}'), m, n=1, \dots, M\}$ defined on S .

It should be pointed out that 2D discretizations required to solve the above equations in real cases (grounding grids) imply an extremely large number

of degrees of freedom. Taking into account that the coefficients matrix in Eq. (1) is not sparse, and that 2D integration in Eq. (1) must be performed twice over the electrode surface, some reasonable simplifications must be introduced to reduce computational cost under an acceptable level.

B. Approximated 1D BEM

It is reasonable to suppose that the leakage current density is constant around the cross section of the cylindrical electrode [32-35], and seems not restrictive whatsoever if we take into account the real geometry of the grounding grids.

Let l be the whole set of axial lines of the buried conductors; let $\hat{r} \in l$ be the orthogonal projection of a generic point $\bar{r} \in S$; let $D(\hat{r})$ be the conductor diameter and suppose all diameters of the conductor segments are the same; and let $J(\hat{r})$ be the approximated leakage current density at this point (assumed uniform around the cross section) in each segment, we can have

$$\phi_j(\bar{r}) = \sum_{i=1}^{N_l} \int_{l_j} \tilde{G}_\phi(\bar{r}, \hat{r}') J_i(\hat{r}') D(\hat{r}') dt_i, \quad (2)$$

where $j=1, \dots, N_s$ and the Green's function of a point current source within the half infinite homogenous earth model is

$$\tilde{G}_\phi(\bar{r}, \hat{r}') = \frac{1}{4\sigma_1} \left(\frac{1}{\bar{R}} - \frac{k_{01}}{\bar{R}'} \right). \quad (3)$$

$\tilde{G}_\phi(\bar{r}, \hat{r}')$ is the average of kernel $G_\phi(\bar{r}, \bar{r}')$ around the cross-section at \hat{r}' [25], $\bar{\sigma}_1 = \sigma_1 + j\omega\epsilon_1$ is the complex conductivity of the homogenous earth.

As the leakage current is not really uniform around the cross-section, variational equality Eq. (1) does not hold anymore if we use Eq. (2). Therefore, it is necessary to restrict the class of weighting functions to those with circumferential uniformity, obtaining

$$\begin{aligned} & \int_{l_j} W(\hat{r}) \varphi_j(\hat{r}) D(\hat{r}) dt_j \\ &= \sum_{i=1}^{N_l} \int_{l_i} W(\hat{r}) \int_{l_i'} \hat{G}_\phi(\hat{r}, \hat{r}') J(\hat{r}') D(\hat{r}') dt_i' D(\hat{r}) dt_j, \end{aligned} \quad (4)$$

where $j=1, \dots, N_l$, dt_i and dt_j lie on l_i and l_j , respectively. For all members $W(\hat{r})$ of a suitable class of weighting functions on l , $\hat{G}_\phi(\hat{r}, \hat{r}')$ is the average of kernel $G_\phi(\bar{r}, \bar{r}')$

around cross sections at \hat{r} and \hat{r}' [25]. The Green's function of a point current source within the half infinite homogenous earth model is

$$\hat{G}_\phi(\hat{r}, \hat{r}') = \frac{1}{4\bar{\sigma}_1} \left(\frac{1}{\hat{R}} - \frac{k_{01}}{\hat{R}'} \right). \quad (5)$$

For a given set of 1D boundary elements $\{l^i; i=1, \dots, N_l\}$ and basis functions $\{N_{l_i}(\hat{r}), i=1, \dots, M\}$ defined on l , the whole set of axial lines of the buried conductors l and the unknown leakage current density $J_l(\hat{r})$ of each segment can be discretized as

$$J_l(\hat{r}) = \sum_{i=1}^M J_{l_i}(\hat{r}), \quad (6)$$

$$l = \bigcup_{i=1}^{N_l} l_i. \quad (7)$$

Finally, for a given set $\{W_{l_j}(\hat{r}); j=1, \dots, M\}$ of weighting functions defined on l , variational statement of Eq. (4) is reduced to a linear equations system:

$$\begin{aligned} & \int_{l_j} \sum_{m=1}^M W_{l_m}(\hat{r}) \phi_j(\hat{r}) dt_j \\ & = \sum_{i=1}^{N_l} \int_{l_i} \sum_{m=1}^M W_{l_m}(\bar{r}) \int_{l_i} \hat{G}_\phi(\hat{r}, \hat{r}') \sum_{n=1}^M J_{l_n} N_{l_n}(\bar{r}') dt'_i dt_j, \end{aligned} \quad (8)$$

where $j=1, \dots, N_l$.

To apply a Galerkin-type of the BEM, we use Galerkin's weighting approach (weighting functions are identical to basis functions), $W_{l_i}(\hat{r}) = N_{l_i}(\hat{r})$, not like [29], which supposes that the current density $J_{l_i}(\hat{r})$ ($i=1, \dots, N_l$) uniformly emanates from the surface of each segment, in order to improve that of the numerical result's precision, here one order basis function is used, and set $M=2$,

$$\sum_{i=1}^2 J_{l_i} N_{l_i}(\hat{r}) = \begin{bmatrix} t_i & 1 \\ l_i & l_i \end{bmatrix} \begin{bmatrix} J_{l_i}^1 \\ J_{l_i}^0 \end{bmatrix} = \frac{J_{l_i}^1}{l_i} t_i + \frac{J_{l_i}^0}{l_i}. \quad (9)$$

Thus, we have

$$\int_{l_j} \begin{bmatrix} t_j \\ l_j \\ 1 \\ l_j \end{bmatrix} \phi_j dt = \sum_{i=1}^{N_l} \int_{l_i} \begin{bmatrix} t_j \\ l_j \\ 1 \\ l_j \end{bmatrix} \int_{l_i} \hat{G}_\phi(\hat{r}, \hat{r}') \begin{bmatrix} t_i & t_i \\ l_i & l_i \end{bmatrix} \begin{bmatrix} J_{l_i}^1 \\ J_{l_i}^0 \end{bmatrix} dt_i dt_j. \quad (10)$$

Furthermore,

$$\begin{bmatrix} l_j^2 \\ 2 \\ 1 \end{bmatrix} \phi_j = \sum_{i=1}^{N_l} \frac{1}{l_j} \int_{l_i} \frac{1}{l_i} \int_{l_i} \hat{G}_\phi(\hat{r}, \hat{r}') \begin{bmatrix} t_j t_i & t_j \\ t_i & 1 \end{bmatrix} \begin{bmatrix} J_{l_i}^1 \\ J_{l_i}^0 \end{bmatrix} dt_i dt_j, \quad (11)$$

where $j=1, \dots, N_l$. The coefficient matrix in the linear system Eq. (11) is symmetric and positive definite [36].

The SEP at any point can be calculated by all leakage currents.

$$\phi_j(\bar{r}) = \sum_{i=1}^{N_l} \int_{l_i} \tilde{G}_\phi(\bar{r}, \hat{r}') \left(\frac{J_{l_i}^1}{l_i} t_i + \frac{J_{l_i}^0}{l_i} \right) dt_i, \quad (12)$$

where $j=1, \dots, N_s$.

Extensive computing is still required to evaluate the averaged kernels $\tilde{G}_\phi(\bar{r}, \hat{r}')$ and $\hat{G}_\phi(\hat{r}, \hat{r}')$ by means of circumferential integration around cross sections at point \hat{r} for $\tilde{G}_\phi(\bar{r}, \hat{r}')$ and at points \hat{r} and \hat{r}' for $\hat{G}_\phi(\hat{r}, \hat{r}')$. The circumferential integration can be avoided by means of the following approximations [25]

$$\hat{R} = \sqrt{(\hat{r} - \hat{r}')^2 + \frac{D(\hat{r}')^2}{4}} = \sqrt{(\hat{r} - \hat{r}')^2 + \frac{D^2}{4}}, \quad (13)$$

$$\tilde{R} = \sqrt{(\hat{r} - \hat{r}')^2 + \frac{D(\hat{r})^2 + D(\hat{r}')^2}{4}} = \sqrt{(\hat{r} - \hat{r}')^2 + \frac{D^2}{2}}. \quad (14)$$

Let the total leakage current from grounding system be I_0 , and the total current into and out of the floating electrode be zero.

For simple expression, we just consider there is only a grounding system and no floating electrode there, the equation system can be expanded as:

$$\begin{bmatrix} Z_{1,1}^{11} & \cdots & Z_{1,N_f}^{11} & Z_{1,1}^{10} & \cdots & Z_{1,N_f}^{10} & -\frac{l_1}{2} \\ \vdots & \vdots & \vdots & \vdots & \vdots & \vdots & \vdots \\ Z_{N_f,1}^{11} & \cdots & Z_{N_f,N_f}^{11} & Z_{N_f,1}^{10} & \cdots & Z_{N_f,N_f}^{10} & -\frac{l_{N_f}}{2} \\ Z_{1,1}^{01} & \cdots & Z_{1,N_f}^{01} & Z_{N_f,1}^{00} & \cdots & Z_{1,N_f}^{00} & -1 \\ \vdots & \vdots & \vdots & \vdots & \vdots & \vdots & \vdots \\ Z_{N_f,1}^{01} & \cdots & Z_{N_f,N_f}^{01} & Z_{N_f,N_f}^{00} & \cdots & Z_{N_f,N_f}^{00} & -1 \\ \frac{l_1}{2} & \cdots & \frac{l_{N_f}}{2} & 1 & \cdots & 1 & 0 \end{bmatrix} \begin{bmatrix} J_{l_1}^1 \\ \vdots \\ J_{l_{N_f}}^1 \\ J_{l_1}^0 \\ \vdots \\ J_{l_{N_f}}^0 \\ \phi_1 \end{bmatrix} = \begin{bmatrix} 0 \\ \vdots \\ 0 \\ 0 \\ \vdots \\ 0 \\ I_0 \end{bmatrix}, \quad (15)$$

where $Z_{ij,(i,j=1,\dots,N_f)}^{nm,(n,m=0,1,l)}$ is the mutual impedance coefficient between a pair of segments with J^n or J^m in grounding system, $J_{l_i,(i=1,\dots,N_f)}^{n,(n=0,1,l)}$ are currents with J^n emanating from the grounding system, ϕ_1 is the SEP of the grounding system. If floating electrodes existed, we can deal with it in the same way.

Supposing the total grounding currents I_0 emanating from the grounding system are known, the leakage current of each segment and the SEP of the grounding system and floating electrode can be obtained by solving Eq. (15). The SEP at any point can then be calculated by the known currents. The grounding impedance and admittance are given by the relation

$$Z_g = \frac{1}{Y_g} = \frac{\phi_1}{I_0} = R_g + jX_g. \quad (16)$$

The element $Z_{ij,(i,j=1,\dots,N_f)}^{nm,(n,m=0,1,l)}$ is defined as

$$Z_{ij}^{nm} = \frac{1}{l_i l_j} \int_{l_i} \int_{l_j} \hat{G}_\phi(\hat{r}, \hat{r}') t_i^m dt_i t_j^n dt_j. \quad (17)$$

For a semi-infinite, homogenous earth model, we have

$$Z_{ij}^{nm} = \frac{1}{l_i l_j} \int_{l_i} \int_{l_j} \left(\frac{1}{\hat{R}} - \frac{k_{01}}{\hat{R}'} \right) t_i^m dt_i t_j^n dt_j. \quad (18)$$

III. THE GREEN'S FUNCTIONS

The main task of simulating grounding systems is to calculate the mutual impedance coefficients shown in Eq. (17). If the earth is a half infinite homogenous conductive medium, Eq. (18) will be calculated easily. However, as the earth is sometimes regarded as a horizontal or vertical multilayer conductive medium in practice, an infinite integral about Bessel function in the Green's function must be calculated, and some fast calculation techniques must be adopted to avoid the integral. As the result, the corresponding closed form of Green's function of a point source in the vertical multilayer earth model must be defined. In order to explain the Green's function of a vertical multilayer earth model, we will explain the Green's function of a horizontal multilayer earth model first.

A. Horizontal multilayer earth model

Considering the low frequency (50 or 60 Hz and higher harmonic wave) and limited size of the substation, the electromagnetic wave's propagating effect can be neglected, so the electromagnetic field can be regarded as a quasi-static electrical field, in this way, the SEP ϕ of a point source with unit current δ buried in a horizontal multilayer earth model satisfies the Poisson equation, supposing the point source is located at the origin of the coordinate system (Fig. 1), the Poisson equation can be expressed as:

$$\nabla^2 \phi_{ij}(x, y, z) = -\frac{\delta(x)\delta(y)\delta(z)\zeta(ij)}{\bar{\sigma}_i}, \quad (19)$$

$$\phi_{ij}(x, y, z) = \phi_{i(j+1)}(x, y, z), \quad (20)$$

$$\bar{\sigma}_j \frac{d\phi_{ij}(x, y, z)}{dz} = \bar{\sigma}_{j+1} \frac{d\phi_{i(j+1)}(x, y, z)}{dz}, \quad (21)$$

where $\bar{\sigma}_i$ is the complex conductivity of i th layer soil, and δ is the Dirac delta function. The subscript i represents the medium in which the unit current is located, and j is the medium in which the SEP is calculated. $\zeta(ij)$ is Kronecker's symbol.

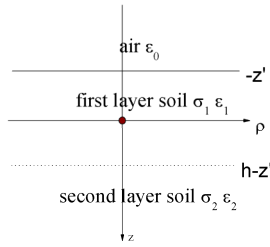


Fig. 1. A scalar point source buried in a horizontal 2-layer earth model.

The procedure for the closed form of the Green's function of a point source in an arbitrary horizontal multilayer earth model can be referred in [29].

Here, two layer earth models are used as an example, according to the procedure in [29], the expression of G_{11} can be given as follows:

$$G_{11}(x, y, z) = \frac{1}{4\pi\bar{\sigma}_1} \int_0^\infty [e^{-k_\rho|z|} - k_{01}e^{-k_\rho(2z'+z)} + f(k_\rho)(k_{01}^2k_{12}e^{-k_\rho(2h+2z'+z)} - k_{01}k_{12}e^{-k_\rho(2h+z)} + k_{12}e^{-k_\rho(2h-2z'-z)} - k_{01}k_{12}e^{-k_\rho(2h-z)})]J_0(k_\rho\rho)dk_\rho, \quad (22)$$

where $f(k_\rho) = \frac{1}{1 + k_{01}k_{12}e^{-k_\rho 2h}}$, $k_{01} = \frac{\bar{\sigma}_0 - \bar{\sigma}_1}{\bar{\sigma}_0 + \bar{\sigma}_1}$,

$k_{12} = \frac{\bar{\sigma}_1 - \bar{\sigma}_2}{\bar{\sigma}_1 + \bar{\sigma}_2}$, h is the thickness of the top earth

layer. $\bar{\sigma}_0$, $\bar{\sigma}_1$, and $\bar{\sigma}_2$ are the complex conductivity of air and two-layer earth, respectively.

In order to avoid Maclaurin's infinite series, we can develop the $f(k_\rho)$ as an exponential series with finite terms by the MP approach as follows [38]:

$$f(k_\rho) = \sum_{i=1}^M \alpha_i e^{\beta_i k_\rho}, \quad (23)$$

where α_i and β_i are constants to be determined by choosing sample points of function $f(k_\rho)$. The MP approach can give highly accurate results with only a few terms, usually four terms, once $f(k_\rho)$ is a monotonic function. How to achieve the exponential series with finite terms by MP can further refer to the appendix part. By employing

the development expression of $f(k_\rho)$ Eq. (23) and the Lipschitz integration, we can obtain

$$G_{11}(x, y, z) = \frac{1}{4\pi\bar{\sigma}_1} \left[\frac{1}{R_0} - \frac{k_{01}}{R'_0} + \sum_{i=1}^M \alpha_i \left(\frac{k_{01}^2 k_{12}}{R_{i1}} - \frac{k_{01} k_{12}}{R_{i2}} + \frac{k_{12}}{R_{i3}} - \frac{k_{01} k_{12}}{R_{i4}} \right) \right], \quad (24)$$

where the origin of the coordinate system shown in Fig. 1 has been moved to the surface between air and earth, and the source point at $(0, z')$, and the field point at (ρ, z') , so $R_0 = \sqrt{\rho^2 + (z - z')^2}$,

$R'_0 = \sqrt{\rho^2 + (z + z')^2}$,

$R_{i(1-4)} = \sqrt{\rho^2 + (\text{sign}_a \cdot z + \text{sign}_b \cdot z' + z_i)^2}$. in which

$\text{sign}_a = 1$ and $\text{sign}_b = -1$ for R_{i1} and R_{i3} ,

$\text{sign}_a = -1$ and $\text{sign}_b = 1$ for R_{i2} and R_{i4} ,

$\text{sign}_a = \text{sign}_b = 1$ for others, $z_i = 2h - \beta_i$.

Each term except $\frac{1}{R_0}$ of Eq. (24) can be

regarded as an image point source, whose location is indicated by R_i and amplitude by α_i . However,

R_i and α_i in Eq. (24) are complex numbers, and the electromagnetic field here was regarded as a quasi-static electrical field so that this approach is named the QSCIM.

Similarly, we can get G_{11} and G_{12} .

B. Vertical multilayer earth model

Just like a point source buried in a horizontal multilayer earth model, here the SEP φ of a point source with unit current δ buried in a vertical multilayer earth model also satisfies the Poisson equation, as we can see in Fig. 2, here we choose the vertical three layers earth model as an example.

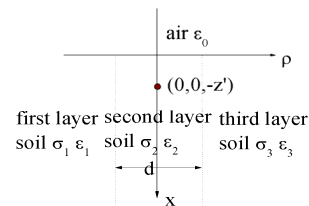


Fig. 2. A scalar point source buried in a vertical, 3-layer earth model.

First, an image point source $\delta' = -k_{12}\delta$ ($0,0,-z'$) can be found in air opposite to the point source δ ($0,0,z'$), which can be seen in Fig. 3(a), in this way, vertical three-layer medium is full of the air. Second, the coordinate axes ρ is inverted from the right direction to the left direction. Then, the coordinate axes ρ is anticlockwise circumvolved downwards with 90 degrees. Last, we can reset the coordinate axes x instead of old ρ and new ρ instead of z , which can be seen in Fig. 3(b).

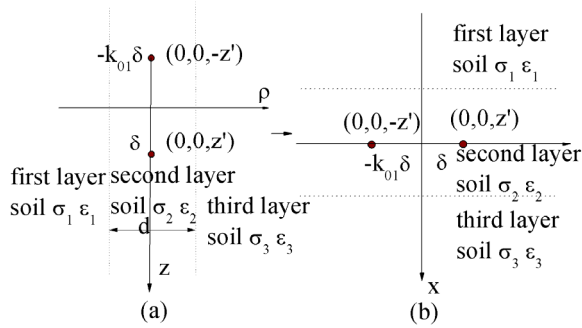


Fig. 3. How to transform the vertical, 3-layer earth model into a horizontal model.

From Fig. 3(b), we can see that each point source δ or δ' can be considered to be buried in a horizontal three layer conductive medium, just like the point source in Fig. 1; so Green's function of point source δ or δ' can be gotten just like the one buried in the horizontal three layer conductive media model. Apply the theory of superposition; the Green's function of a point source buried in the vertical three layer earth model can be gotten.

$$G_{22}(r, r') = \frac{1}{4\pi\sigma_1} \left\{ \frac{1}{R_{00}} - \frac{k_{12}}{R_{00}} - \frac{k_{01}}{R'_{00}} + \frac{k_{01}k_{12}}{R'_{01}} \right. \\ \left. + \sum_{i=1}^M \alpha_n \left[\left(\frac{k_{23}}{R_{i1}} - \frac{k_{12}k_{23}}{R_{i2}} - \frac{k_{12}k_{23}}{R_{i3}} - \frac{k_{12}}{R_{i4}} \right) \right. \right. \\ \left. \left. - k_{01} \left(\frac{k_{23}}{R'_{i1}} - \frac{k_{12}k_{23}}{R'_{i2}} - \frac{k_{12}k_{23}}{R'_{i3}} - \frac{k_{12}}{R'_{i4}} \right) \right] \right\}, \quad (22)$$

where R_{00} and R'_{00} are same as tR_0 and R'_0 of Eq. (24),

$$R_{01} = \sqrt{(x+x')^2 + (y-y')^2 + (z-z')^2},$$

$$R'_{01} = \sqrt{(x+x')^2 + (y-y')^2 + (z+z')^2},$$

$$R_{i(i-4)} = \sqrt{(\text{sign}_a \cdot x + \text{sign}_b \cdot x' + x_i)^2 + (y-y')^2 + (z-z')^2},$$

and

$$R'_{i(i-4)} = \sqrt{(\text{sign}_a \cdot x + \text{sign}_b \cdot x' + x_i)^2 + (y-y')^2 + (z+z')^2}.$$

The signs are $\text{sign}_a = 1$ and $\text{sign}_b = -1$ for R_{i1} and R_{i3} , $\text{sign}_a = -1$ and $\text{sign}_b = 1$ for R_{i3} and R_{i4} , and $\text{sign}_a = \text{sign}_b = 1$ for others, $x_i = 2h - \beta_i$. Note that

here $f(k_\rho) = \frac{1}{1 + k_{12}k_{23}e^{-k_\rho 2h}}$ has been expanded

into the finite exponential terms series, which is different from the one of horizontal multilayer earth model. Meanwhile, when the two layers vertical earth model is considered, the complex images of the point source will disappear. This is also different from the one of the horizontal multilayer earth model.

Similarly, we can get G_{21} , G_{23} , G_{11} , G_{12} , G_{13} , G_{31} , G_{32} and G_{33} . The Green's function of a point source buried in the arbitrary vertical multilayer earth model can be achieved in a similar way.

Once the closed form of Green's function of a point source in the vertical multilayer earth model has been derived, the mutual impedance coefficient can be fastly calculated through Eq. (17). It should be pointed out that the integral of Eq. (17) can be analytically calculated with the closed form of Green's function, for 0 order ($n=0, m=0$) term, which is described in [24], and one order ($n=0, m=1; n=1, m=0; n=1, m=1$) terms can refer to [25].

IV. SIMULATION RESULTS AND ANALYSIS

According to the approach introduced in this paper, a FORTRAN language program has been implemented; the program can simulate a grounding system and up to the vertical three-layer earth model.

A. Verification of the approach

To verify the result of the method proposed in this work, some cases solved by other authors are studied.

The first case, from [28], is a horizontal grounding electrode of 20m length and 0.16m radius, buried at $l_0 = 1m$ depth in the vertical,

three-layer earth, where $p_{21} = \frac{\bar{\sigma}_2}{\bar{\sigma}_1}$, $p_{32} = \frac{\bar{\sigma}_3}{\bar{\sigma}_2}$, $\sigma_1 = 0.01 S/m$, $\varepsilon_1 = 81\varepsilon_0$, $\varepsilon_2 = 5\varepsilon_0$, $\varepsilon_3 = 2\varepsilon_0$, $d = 3m$, $f = 50Hz$, and $I_e = 300A$, which can be seen in Fig. 4.

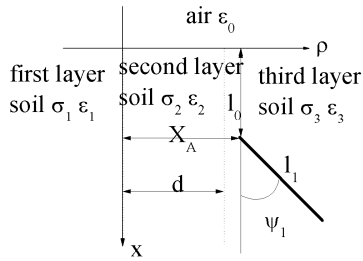


Fig. 4. Configuration of a simulated grounding conductor.

There are two results in [19]: (1) $X_A = d + 1 = h + 1 = 4m$, $\theta_1 = 90^\circ$, and $\psi_1 = 0^\circ$, the result can be seen in Table I; and (2) $X_A = d + 1 = h + 1$, $\theta_1 = \psi_1 = 90^\circ$, the result can be seen in Tables 2 and 3.

The second case also comes from [28], which can also be seen in Fig. 4. The vertical three-layer earth model is considered, whose left layer soil's conductivity and permittivity are $\sigma_1 = \sigma_0 = 0.0 S/m$ and $\varepsilon_1 = \varepsilon_0$, the middle layer soil's conductivity and permittivity are $\sigma_2 = 1000.0^{-1} S/m$ and $\varepsilon_2 = 5\varepsilon_0$, its thickness is $d = 1.5m$, the right layer soil's conductivity and permittivity are $\sigma_3 = 250.1^{-1} S/m$ and $\varepsilon_3 = 9\varepsilon_0$, a horizontal grounding electrode of $l_1 = 20m$ length and $9.23mm$ radius and buried at $l_0 = 1m$ depth in the vertical three-layer earth is chosen. Other parameters are $X_A = 4.5m$, $Y_A = 0.0m$, $f = 50Hz$, and $\theta_1 = 90^\circ$. Good agreements can be seen in Table 4.

B. The computational cost and accuracy of the approach

First, by considering some reasonable simplification, the approach calculates the grounding system based on the 1D Galerkin type

of BEM. Second, the main task of simulating grounding system is to calculate the mutual

Table 1: Comparison of our results $Z_g(\Omega)$ with a published model: $p_{21} = 0.01$ and $p_{32} = 10.0$

| Ref. [9] | Zero-order function | One-order function |
|---------------|---------------------|--------------------|
| 5.30-j7.17e-6 | 5.37-j7.74e-6 | 5.37-j7.72e-5 |

Table 2: Comparison of our results $Z_g(\Omega)$ with a published model: $p_{21} = 0.01$ and $p_{32} = 10.0$

| h | Ref. [9] | Zero-order function | One-order function |
|------|----------------|---------------------|--------------------|
| 0 | 2.77-j5.34e-6 | 2.75-j2.42e-6 | 2.75-j2.41e-6 |
| 1e-3 | 2.78-j2.56e-6 | 2.34-j4.14e-6 | 2.34-j4.14e-6 |
| 1e-1 | 3.45-j9.75e-6 | 3.24-j12.89e-6 | 3.24-j12.88e-6 |
| 1e-0 | 5.44-j17.83e-6 | 5.67-j21.18e-6 | 5.67-j21.19e-6 |
| 1e1 | 7.23-j13.54e-6 | 7.58-j15.11e-6 | 7.58-j15.12e-6 |
| 1e3 | 7.72-j11.88e-6 | 7.99-j11.99e-6 | 7.99-j11.98e-6 |
| 1e5 | 7.70-j11.01e-6 | 8.00-j11.95e-6 | 8.00-j11.97e-6 |

Table 3: Comparison of our results $Z_g(\Omega)$ with a published model: $p_{21} = 100.0$ and $p_{32} = 0.1$

| h | Ref. [9] | Zero-order function | One-order function |
|------|-----------------|---------------------|--------------------|
| 0 | 7.70-j115.34e-6 | 7.80-j135.55e-6 | 7.80-j135.54e-6 |
| 1e-3 | 7.69-j130.01e-6 | 8.20-j152.16e-6 | 8.20-j152.15e-6 |
| 1e-1 | 7.04-j104.27e-6 | 7.30-j118.11e-6 | 7.30-j118.12e-6 |
| 1e-0 | 5.06-j46.46e-6 | 4.87-j49.01e-6 | 4.87-j49.02e-6 |
| 1e1 | 3.25-j11.27e-6 | 2.96-j10.11e-6 | 2.96-j10.10e-6 |
| 1e3 | 2.81-j4.65e-6 | 2.55-j2.94e-6 | 2.55-j2.93e-6 |
| 1e5 | 2.77-j4.28e-6 | 2.54-j2.87e-6 | 2.54-j2.86e-6 |

Table 4: Comparison of our results $Z_g(\Omega)$ with a published model [19]

| ψ_1 | Ref. [9] | Zero-order function | One-order function |
|----------|---------------------|---------------------|--------------------|
| 0 | 15.51- j9.84e-5 | 15.12- j9.14e-5 | 15.04- j9.10e-5 |
| 90 | 15.58- j9.90e-5 | 15.16- j9.14e-5 | 15.08- j9.09e-5 |
| 60 | 15.85- j12.82e-5 | 15.32- j9.16e-5 | 15.24- j9.16e-5 |
| 90 | 16.82- j12.29e-5 | 15.96- j9.34e-5 | 15.96- j9.34e-5 |

impedance coefficients as shown in Eq. (17). Although the multilayer earth model must be considered in a real practice problem, the closed form of Green's function of a point source in the multilayer earth model can be taken to avoid verbose calculation about infinite integral or Maclaurin's series [25-35] by applying the QSCIM. Third, the analytical formula about mutual impedance is adopted to avoid numerical integral in the approach. Therefore, the approach is very fast. For a general real practiced grounding system, it needs only several seconds on a P4 computer. Verification of the approach has been shown in the above section, by comparing our results with those from a different method in other references, especially with measurement data. We can see that the accuracy of our approach is good.

C. Numerical result analysis

A complex grounding system can be seen in Fig. 5. The earth is modeled as a three vertical layers conductive media, whose conductivities and permittivity are $\sigma_1 = 100.0^{-1} S/m$, $\sigma_2 = 800.0^{-1} S/m$, $\sigma_3 = 300.0^{-1} S/m$, $\epsilon_1 = 5\epsilon_0$, $\epsilon_2 = 12\epsilon_0$, and $\epsilon_3 = 10\epsilon_0$. The middle layer's thickness is $d = 5m$. All the conductors' radius of grid is 10mm, and rods' radius of 16mm. The external excited AC current 1000A of current with power frequency (50Hz) is injected from the corner of the grounding system.

The calculated numerical results can be seen in Table 5. Note: Z_g is the grounding impedance; GPR_g is the grounding potential rise (GPR) of the grounding grid; SEP_f is the SEP of the floating grid; I_0 is the total leakage current of the

grounding system; and if is the total net current flowing into and out of the floating grid.

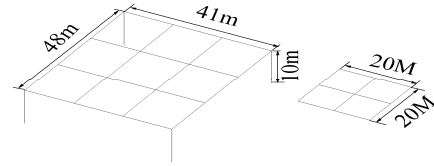


Fig. 5. Grounding system and floating grid.

Table 5: Numerical results

| | f=50Hz case | f=800Hz case |
|---------------|------------------|-----------------|
| $Z_g(\Omega)$ | 1.78-j0.62e-5 | 1.78-j0.99e-4 |
| $GPR_g(V)$ | 1775.74-j6.e-3 | 1775.74-j003 |
| $SEP_f(V)$ | 437.19-j2.e-3 | 437.18-j0.03 |
| $I_0(A)$ | 100.0-j1.24e-10 | 100.0+j3.26e-9 |
| $I_f(A)$ | -1.9e-6+j2.9e-11 | 1.7e-6-j5.8e-10 |

It can be seen that the total leakage current of the grounding system is close to the external injected current and net current flowing into and out of the small grid is near zero. All these verify the accuracy of this model.

The 3D distribution of SEP's absolute value along the earth surface is given in Fig. 6, and the 3D distribution of step voltage's absolute value along the earth surface is given in Fig. 7.

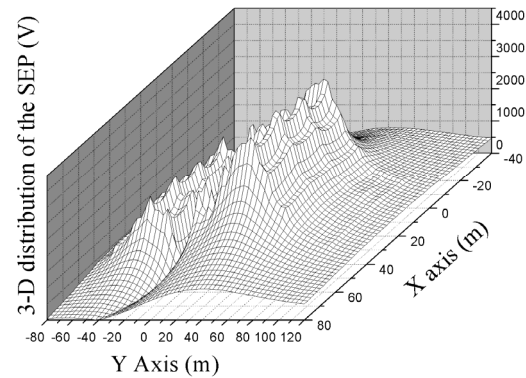


Fig. 6. The 3D distribution of the SEP absolute value for a vertical, three-layer earth model, obtained by the QSCIM.

It can be seen from Fig. 6, that (1) the SEP rise of the surface above the grounding grid is much higher, meanwhile, the distribution has been divided into three parts. This is because an external excited AC current was injected from the

grounding grid; the vertical three layer earth model has re-distribution of the leakage current along the grid. (2) the GPR is centralized above the grounding grid, the ground surface's SEP becomes lower around the grounding grid, meanwhile, the GPR along the interface between the different vertical layer earth has become small, so the step voltage will become bigger, the large value of step voltage is distributed around the earth surface above the edge of the grounding grid and the interface, which can be seen from Fig. 7. So some safety measures must be taken to mitigate the question.

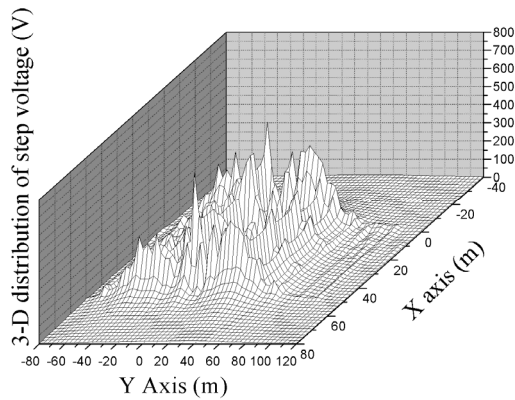


Fig. 7. The 3D distribution of the step voltage absolute value for a vertical, three-layer earth model, obtained by the QSCIM.

V. CONCLUSION

1. The quasi-static complex image approach is very efficient to simulate the grounding grids in vertical multilayer earth models. Usually, few quasi-static complex images can provide accurate simulation results.
2. Novel closed form of Green's functions for vertical multilayered earth model achieved by the method of quasi-static complex images have been introduced in this paper.
3. Linear basis function has succeeded in being realized in the BEM for simulating grounding systems.
4. A program based on Galerkin's BEM has been developed for simulating grounding systems with any complicated structure buried in up to the vertical three-layer earth models.

APPENDIX: THE QSCIM BASED ON MP METHOD

The QSCIM can be implemented with a MP approach. The MP approach is approximating a function by a sum of complex exponentials, and works well once the function monotonically decays.

From [38] and [39], if a function $f(x)$ can be expanded into finite exponential series, as below

$$f(x) = \sum_{i=1}^M \alpha_i e^{\beta_i x}. \quad (26)$$

There are three parameters to be decided, such as M , α_i , and β_i .

In order to get these parameters, we first decide maximum sample points according to the characteristic of function $f(x)$, that means maximum value for x_{\max} can be obtained. Once x_{\max} has been known, we can get uniformly discrete values of $f(x)$ within scope $(0 \leq x \leq x_{\max})$. So, we have uniform discrete function values of $f(x)$ with $(f(0), f(1), f(2), \dots, f(N-1))$ corresponding to value of x as $(0, \Delta x, 2\Delta x, \dots, (N-1)\Delta x)$ or $(0, x_1, x_2, \dots, x_{\max})$. Here, Δx is the rate of sampling. We can obtain

$$f(x) \approx \sum_{i=1}^M \alpha_i z_i^k \quad (k=0, \dots, N-1), \quad (27)$$

where

$$z_i^k = e^{\beta_i \Delta x k} \quad (i=0, \dots, M). \quad (28)$$

A. How to decide the number M

Since, we have the total N number of uniform discrete function values of $f(x)$, we can get the matrix $[Y]$ from the sampling data $f(x)$ by combining $[Y_1]$ and $[Y_2]$ as

$$[Y] = \begin{bmatrix} f(0) & f(1) & \dots & f(L-1) \\ f(1) & f(2) & \dots & f(L+1) \\ \vdots & \vdots & \dots & \vdots \\ f(N-L-1) & f(N-L) & \dots & f(N-1) \end{bmatrix}_{(N-L) \times (L+1)}, \quad (29)$$

$$[Y_1] = \begin{bmatrix} f(0) & f(1) & \cdots & f(L-1) \\ f(1) & f(2) & \cdots & f(L) \\ \vdots & \vdots & \cdots & \vdots \\ f(N-L-1) & f(N-L) & \cdots & f(N-2) \end{bmatrix}_{(N-L) \times L}, \quad (30)$$

$$[Y_2] = \begin{bmatrix} f(1) & f(2) & \cdots & f(L) \\ f(2) & f(3) & \cdots & f(L+1) \\ \vdots & \vdots & \cdots & \vdots \\ f(N-L) & f(N-L+1) & \cdots & f(N-1) \end{bmatrix}_{(N-L) \times L}, \quad (31)$$

where L is referred to as the pencil parameter [38] and [39].

Note that $[Y_1]$ is obtained from $[Y]$ by omitting the last column, and $[Y_2]$ is obtained from $[Y]$ by omitting the first column. The parameter L can be chosen between $N/3$ and $N/2$.

Next, singular-value decomposition (SVD) of the matrix $[Y]$ can be implemented out as

$$[Y] = [U][\Sigma][V]^H, \quad (32)$$

where $[U]$ and $[V]$ are unitary matrices, comprised of the eigenvector of $[Y][Y]^H$ and $[Y]^H[Y]$, respectively, and $[\Sigma]$ is a diagonal matrix including the singular values of $[Y]$, i. e.

$$[U]^H[Y][V] = [\Sigma]. \quad (33)$$

The choice of the parameter M can be achieved at this stage by studying the ratios of various singular values to the largest one. Typically, the singular values beyond M are set equal to zero. The way M is chosen is as follows. Observe the singular value σ_c such that

$$\frac{\sigma_c}{\sigma_{\max}} \approx 10^{-p}, \quad (34)$$

where p is the number of significant decimal digits in the data. For example, if the sampling data is accurate up to three significant digits, the singular values for which the ratio in Eq. (34) is below 10^{-3} are essentially useless singular values, and they should not be used in the reconstruction of the sampling data.

We next introduce the ‘‘filtered’’ matrix, $[V']$, constructed so that it contains only M predominant right-singular vectors of $[V]$;

$$[V'] = [v_1, v_2, \dots, v_M]. \quad (35)$$

The right-singular vectors from $M+1$ to L , corresponding to the small singular values, are omitted. Therefore,

$$[Y_1] = [U][\Sigma][V'_1]^H, \quad (36)$$

$$[Y_2] = [U][\Sigma][V'_2]^H, \quad (37)$$

where $[V'_1]$ is obtained from $[V']$ with the last row of $[V']$ omitted, $[V'_2]$ is obtained by deleting the first row of $[V']$; and $[\Sigma']$ is obtained from the M columns of $[\Sigma]$ corresponding to the M predominant singular values.

B. How to decide β_i

To motivate the MP method, we can use the two $(N-L) \times L$ matrices, Y_1 and Y_2 . We can rewrite

$$[Y_2] = [Z_1][R][Z_0][Z_2], \quad (38)$$

$$[Y_1] = [Z_1][R][Z_2], \quad (39)$$

where

$$[Z_1] = \begin{bmatrix} 1 & 1 & \cdots & 1 \\ z_1 & z_2 & \cdots & z_M \\ \vdots & \vdots & \cdots & \vdots \\ z_1^{N-L-1} & z_2^{N-L-1} & \cdots & z_M^{N-L-1} \end{bmatrix}_{(N-L) \times M}, \quad (40)$$

$$[Z_2] = \begin{bmatrix} 1 & z_1 & \cdots & z_1^{L-1} \\ 1 & z_2 & \cdots & z_2^{L-1} \\ \vdots & \vdots & \cdots & \vdots \\ 1 & z_M & \cdots & z_M^{L-1} \end{bmatrix}_{M \times L}, \quad (41)$$

$$[Z_0] = \text{diag}[z_1, z_2, \dots, z_M], \quad (42)$$

$$[R] = \text{diag}[R_1, R_2, \dots, R_M], \quad (43)$$

where $\text{diag}[\bullet]$ represents a $M \times M$ diagonal matrix.

Now, we introduce the matrix pencil

$$[Y_2] - \lambda[Y_1] = [Z_1][R]\{[Z_0] - \lambda[I]\}[Z_2], \quad (44)$$

where $[I]$ is the $M \times M$ identity matrix. We can demonstrate that, in general, the rank of $\{[Y_2] - \lambda[Y_1]\}$ will be M ,

provided $M \leq L \leq N - M$. However, if $\lambda = z_i$, $i = 1, 2, \dots, M$, the i th row of $\{[Z_0] - \lambda[I]\}$ is zero, and the rank of this matrix is $M - 1$. Hence, the parameters z_i , may be found as generalized eigenvalues of the matrix pair $\{[Y_2]; [Y_1]\}$. Equivalently, the problem of solving for z_i can be transformed into an ordinary eigenvalue problem,

$$\{[Y_1]^+[Y_2] - \lambda[I]\}, \quad (45)$$

where $[Y_1]^+$ is Moore-Penrose pseudo-inverse of $[Y_1]$, and is defined as

$$[Y_1]^+ = \{[Y_1]^H [Y_1]\}^{-1} [Y_1]^H, \quad (46)$$

where the superscript "H" denotes the conjugate transpose.

The eigenvalues of the matrix

$$\{[Y_2] - \lambda[Y_1]\}_{L \times M} \Rightarrow \{[Y_1]^+[Y_2] - \lambda[I]\}_{M \times M}, \quad (47)$$

are equivalent to the eigenvalues of the matrix

$$\{[V'_2]^H - \lambda[V'_1]^H\} \Rightarrow \{[V'_1]^+\}^+ \{[V'_2]^H\}^+ - \lambda[I]. \quad (48)$$

This methodology can be used to solve for z_i .

Lastly, we point out that in this case z_i represents β_i .

C. How to decide α_i

Once M and the z_i are known, α_i , are solved with the help of the following least-squares problem:

$$\begin{bmatrix} f(0) \\ f(1) \\ \vdots \\ f(N-1) \end{bmatrix} = \begin{bmatrix} 1 & 1 & \cdots & 1 \\ z_1 & z_2 & \cdots & z_M \\ \vdots & \vdots & \cdots & \vdots \\ z_1^{N-1} & z_2^{N-1} & \cdots & z_M^{N-1} \end{bmatrix} \begin{bmatrix} \alpha_1 \\ \alpha_2 \\ \vdots \\ \alpha_M \end{bmatrix}. \quad (49)$$

D. Example for MP

The kernel of Green's function of point source lying in the vertical multilayer earth model can be expanded into a sum of complex exponential terms. Generally speaking, only a few terms of quasi-static complex images can arrive at a very high precision. We will show merit of this method through the vertical three-layer earth model.

Earth's conductivities and permittivity's are $\sigma_1 = 100.0^{-1} S/m$, $\sigma_2 = 200.0^{-1} S/m$,

$\sigma_3 = 300.0^{-1} S/m$, $\varepsilon_1 = 5\varepsilon_0$, $\varepsilon_2 = 12\varepsilon_0$, and $\varepsilon_3 = 10\varepsilon_0$, respectively. The middle layer earth thickness is $5m$. With the MP approach, only two terms of the quasi-static complex images can arrive at relative error 0.1%. From Fig. 8 and Fig. 9, we can see that the two curves are superposed to each other, the two terms of quasi-static complex images' coefficients are given in Table 6.

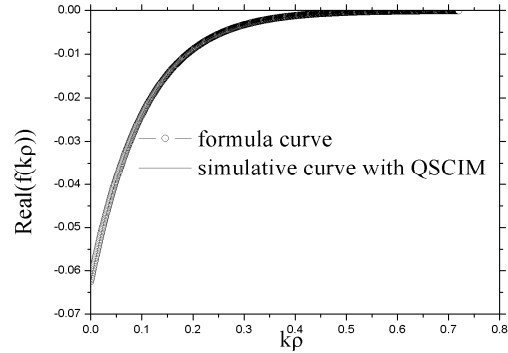


Fig. 8. Two curves from function and simulation (real part).

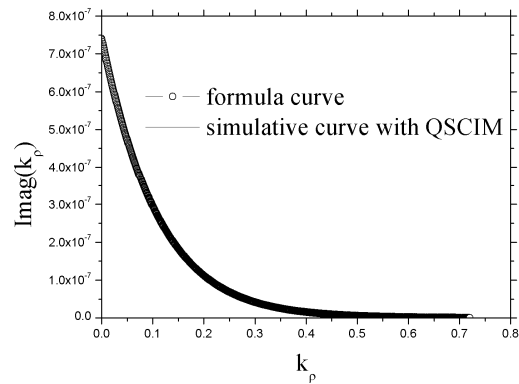


Fig. 9. Two curves from function and simulation (imaginary part).

Table 6: Coefficients of the quasi-static complex images for a vertical, three-layer earth model

| i | α_i | β_i |
|---|--------------------|------------------|
| 1 | 6.692e-2-j7.298e-4 | 10.009-j1.341e-6 |
| 2 | 4.423e-3-j1.451e-3 | 19.027+j3.627e-5 |

ACKNOWLEDGMENT

This work is supported by China Electrical Power Research Institute.

REFERENCES

- [1] M. Mamaoorty, M. M. B. Narayanan, S. Parameswaran, and D. Mukhedkar, "Transient Performance of Grounding Grids," *IEEE Transactions on Power Delivery*, vol. PWRD-4, no. 4, pp. 2053-2059, 1989.
- [2] W. Xiong and F. P. Dawalibi, "Transient Performance of Substation Grounding Systems Subjected to Lightning and Similar Surge Currents," *IEEE Transactions on Power Delivery*, vol. PWRD-9, no. 3, pp. 1412-1420, 1994.
- [3] M. Heimbach and L. D. Grcev, "Grounding System Analysis in Transient Program Applying Electromagnetic Field Approach," *IEEE Transactions on Power Delivery*, vol. PWRD-12, no. 1, pp. 186-193, 1997.
- [4] R. Andolfato, L. Bernardi, and L. Fellin, "Aerial and Grounding System Analysis by the Shifting Complex Images Method," *IEEE Transactions on Power Delivery*, vol. PWRD-15, no. 3, pp. 1001-1009, 2000.
- [5] Y. Q. Liu, N. Theethayi, and R. Thottappillil, "An Engineering Model for Transient Analysis of Grounding System under Lightning Strikes: Nonuniform Transmission Line Approach," *IEEE Transactions on Power Delivery*, vol. PWRD-20, no. 2, pp. 722-730, 2005.
- [6] D. Poljak and V. Doric, "Wire Antenna Model for Transient Analysis of Simple Ground Systems, Part I: The Vertical Grounding Electrode," *Progress In Electromagnetics Research*, vol. PIER 64, pp. 149-166, 2006.
- [7] D. Poljak and V. Doric, "Wire Antenna Model for Transient Analysis of Simple Ground Systems, Part I: The Horizontal Grounding Electrode," *Progress In Electromagnetics Research*, vol. PIER 64, pp. 167-189, 2006.
- [8] M. Osman Goni, E. Kaneko, and A. Ametani, "Finite Difference Time Domain Method for the Analysis of Transient Grounding Resistance of Buried Thin Wires," *ACES Journal*, vol. 22, no. 3, 2007.
- [9] A. F. Otero, J. Cidras, and J. L. Alamo, "Frequency-Dependent Grounding System Calculation by Means of a Conventional Nodal Analysis Technology," *IEEE Transactions on Power Delivery*, vol. PWRD-14, pp. 873-877, 1999.
- [10] F. Dawalibi, "Electromagnetic Fields Generated by Overhead and Buried Short Conductors, Part 2-Ground Network," *IEEE Transactions on Power Delivery*, vol. PWRD-1, pp. 112-119, 1986.
- [11] L. Huang and D. G. Kasten, "Model of Ground Grid and Metallic Conductor Currents in High Voltage A.C. Substations for the Computation of Electromagnetic Fields," *Electric Power Systems Research*, vol. 59, pp. 31-37, 2001.
- [12] H. O. Brodskyn, M. C. Costa, J. R. Cardoso, N. M. Abe, and A. Passaro, "Ground-3D Linked to Line Parameters: A Method to Fault Current Distribution and Earth Potential Determination," *ACES Journal*, vol. 12, no. 1, 1997.
- [13] Z. X. Li, W. J. Chen, J. B. Fan, and J. Y. Lu, "A Novel Mathematical Modeling of Grounding System Buried in Multilayer Earth," *IEEE transactions on Power Delivery*, vol. PWRD-21, pp. 1267-1272, 2006.
- [14] Z. X. Li and W. J. Chen, "Numerical Simulation Grounding System Buried Within Horizontal Multilayer Earth in Frequency Domain," *Communications in Numerical Methods in Engineering*, vol. 23, pp. 11-27, 2007.
- [15] Z. X. Li and J. B. Fan, "Numerical Calculation of Grounding System in Low Frequency Domain Based on Boundary Element Method," *International Journal for Numerical Methods in Engineering*, vol. 73, pp. 685-705, 2008.
- [16] Z. X. Li, J. B. Fan, and W. J. Chen, "Numerical Simulation of Substation Grounding Grids Buried in Both Horizontal and Vertical Multilayer Earth Model," *International Journal for Numerical Methods in Engineering*, vol. 69, pp. 2359-2380, 2007.
- [17] Z. X. Li, G. F. Li, J. B. Fan, and C. X. Zhang, "Numerical Simulation of Grounding System Buried in Vertical Multilayer Earth Model in Low Frequency Domain Based on the Boundary Element Method," *European Transactions on Electrical Power*, vol. 19, pp. 1177-1190, 2009.
- [18] L. Zhang, J. Yuan, and Z. X. Li, "The Complex Image Method and its Application in Numerical Simulation of Substation Grounding Grids," *Communications in*

- Numerical Methods in Engineering*, vol. 15, pp. 835-839, 1999.
- [19] Y. L. Chow, J. J. Yang, and K. D. Srivastava, "Complex Images of a Ground Electrode in Layered Soils," *Journal of Applied Physics*, vol. 71, pp. 569-574, 1992.
- [20] S. Vujevic and M. Kurtovic, "Numerical Analysis of Earthing Grids Buried in Horizontal Stratified Multilayer Earth," *International Journal for Numerical Methods in Engineering*, vol. 41, pp. 1297-1319, 1998.
- [21] Y. L. Chow, M. M. Elsherbiny, and M. M. A. Salama, "Surface Voltages and Resistance of Grounding System of Grid and Rods in Two-Layer Earth by the Rapid Galerkin's Moment Method," *IEEE Transactions on Power Delivery*, vol. PWRD-12, pp. 179-185, 1997.
- [22] A. P. Sakis Meliopoulos, F. Xia, G. J. Cokkinides, "An Advanced Computer Model for Grounding System Analysis," *IEEE Transactions on Power Delivery*, vol. PWRD-8, no. 1, pp. 13-23, 1993.
- [23] L. M. Livshitz, P. D. Einziger, and J. Mizrahi, "A Model of Finite Electrodes in Layered Biological Media: Hybrid Image Series and Moment Method Scheme," *ACES Journal*, vol. 16, no. 2, pp. 145-154, 2001.
- [24] R. J. Hepe, "Computation of Potential at Surface Above an Energized Grid or Other Electrode, Allowing for Non-Uniform Current Distribution," *IEEE Transactions on Power Apparatus and System*, vol. PAS-98, no. 6 pp. 1978-1989, 1979.
- [25] I. Colominas, F. Navarrina, and M. Casteleiro, "A Boundary Element Numerical Approach for Grounding Grid Computation," *Computer Methods in Applied Mechanics and Engineering*, vol. 174, pp. 73-90, 1999.
- [26] U. Adriano, O. Bottauscio, and M. Zucca, "Boundary Element Approach for the Analysis and Design of Grounding Systems in Presence of Non-Homogeneous," *IEE Proceedings on Generation, Distribution and distribution*, vol.150, no. 3, pp. 360-366, 2003.
- [27] P. D. Rancic, L. V. Stefanovic, and D. R. Djordjevic, "An Improved Linear Grounding System Analysis in Two-Layer Earth," *IEEE Transactions on Magnetic*, vol. 32, no. 5, part 3, pp. 5179-5187, 1996.
- [28] P. D. Rancic, L. V. Stefanovic, and D. R. Djordjevic, "Analysis of Linear Ground Electrodes Placed in Vertical Three-Layer Earth," *IEEE Transactions on Magnetic*, vol. 32, no. 3, pp. 1505-1508, 1996.
- [29] Z. X. Li, J. B. Fan, and W. J. Chen, "Numerical Simulation Grounding Grids Buried in Both Horizontal and Vertical Multilayer Earth Model," *International Journal for Numerical Methods in Engineering*, vol. 69, no. 11, pp. 2359-2380, 2007.
- [30] J. R. Wait and K. P. Spies, "On the Representation of the Quasi-Static Fields of a Line Current Source above the Ground," *Canadian Journal of Physics*, vol. 47, pp. 2731-2733, 1969.
- [31] D. J. Thomson, J. T. Weaver, and et. al, "The Complex Image Approximation for Induction in a Multilayer Earth," *Journal of Geophysical Research*, vol. 80, pp. 123-129, 1975.
- [32] J. G. Sverak, W. K. Dick, T. H. Dodds, and R.H. Hepe, "Substations Grounding. Part I," *IEEE Transactions on Power Apparatus and Systems*, vol. PAS-100, no. 9, pp. 4281-4290, 1981.
- [33] J. G. Sverak, W. K. Dick, T. H. Dodds, and R.H. Hepe, "Substations Grounding. Part II," *IEEE Transactions on Power Apparatus and Systems*, vol. PAS-101, no. 10, pp. 4006-4023, 1982.
- [34] D. L. Garrett and J. G. Pruitt, "Problems Encountered with the Average Potential Method of Analyzing Substation Grounding Systems," *IEEE Transactions on Power Apparatus and Systems*, vol. PAS-104, no. 12, pp. 3586-3596, 1985.
- [35] I. Colominas, F. Navarrina, and M. Casteleiro, "A Numerical Formulation for Grounding Analysis in Stratified Soils," *IEEE Transactions on Power Delivery*, vol. PWRD-17, pp. 587-595, 2002.
- [36] C. Johnson, *Numerical Solution of Partial Differential Equations by the Finite Element Method*. Cambridge, U.K.: Cambridge Univ. Press, 1987.
- [37] E. D. Sunde, *Earth Conduction Effects in Transmission Systems*, Dover Pub., New York, 1968.
- [38] R. S. Adve and T. K. Sarkar, "Extrapolation of Time-Domain Responses from Three-Dimensional Conducting Objects Utilizing the Matrix Pencil Technique," *IEEE Transactions*

on *Antenna and Propagation*, vol. AP-45, no. 1, pp. 147-156, 1997.

- [39] T. K. Sakar and O. Pereira, "Using the Matrix Pencil Method to Estimate the Parameters of a Sum of Complex Exponentials," *IEEE antenna and Propagation Magazine*, vol. 37, no. 1, pp. 48-55, February 1995.



Zhong-Xin Li was born in Xi'an, Shaangxi, China. He received the Bachelor's and Master's degree from Xi'an Jiaotong University in 1989 and 1994, respectively, and the Ph.D. degree from Tsinghua University in March 1999.

He joined Fudan University in 1999, first as a Postdoctoral Fellow and then becoming an Associate Professor in 2001. From 2003 to 2004, he was with the Branch of Electromagnetic Environment Research, Electrical Power Research Institute of China. From January 2004 to May 2005, he was with the Department of Electronic Engineering, Hong Kong City University, as a Senior Research Associate. From May 2005 to May 2007, he was an Associate Professor at the Electromagnetic Academy, Zhejiang University. Since May 2007, he has been with the Branch of Overvoltage and Insulation Coordination of the China Electrical Power Research Institute. His special fields of interest included grounding system analysis and high-frequency electromagnetic wave and remote sensing.

Guang-Fan Li received the Master's degree from China Electric Power Research Institute (CEPRI), Beijing, China, in 1983.

He joined CEPRI in 1983, where he is currently the Head of the High Voltage Research Institute. His research interests include ac and dc UHV transmission technology.



Jian-Bin Fan was born in Shanxi Province, China in 1967. He received the B.Sc. and M.Sc. degrees from the Department of Electrical Engineering, Xi'an Jiaotong University, Xi'an China, in 1990 and 1995, respectively. After two years of work in a transformer plant, he studied at China Electric Power Research Institute and received the Ph.D. degree there in 2000.

Currently, he is the Vice Director of High Voltage Department, China Electric Power Research Institute. He is also the Vice Director of Electric Power Industry Quality Inspection & Test Centre. He is the member of IEC SB1 (Electricity transmission and distribution), IEC TC36 WG11, CIGRE B3.22 and so on. He is the Secretary General of National UHV AC Transmission Technology Standardization Committee of China, Vice Secretary General of National HVDC Transmission Technology Standardization Committee of China, and so on. His main research interests include external insulation and operation of high voltage transmission lines and equipment, especially in UHV areas.



Yu Yin was born in March, 1975 in Xi'an city of Shaangxi Province. He graduated from Tsinghua University with Ph.D. in 2004. Since then he joined in the China Electric Power Research Institute. His research interest is high volte technology.